ARTICLE

doi:10.1038/nature17145

Contribution of Antarctica to past and future sea-level rise

Robert M. DeConto[1] & David Pollard[2]

Polar temperatures over the last several million years have, at times, been slightly warmer than today, yet global mean sea level has been 6–9 metres higher as recently as the Last Interglacial (130,000 to 115,000 years ago) and possibly higher during the Pliocene epoch (about three million years ago). In both cases the Antarctic ice sheet has been implicated as the primary contributor, hinting at its future vulnerability. Here we use a model coupling ice sheet and climate dynamics—including previously underappreciated processes linking atmospheric warming with hydrofracturing of buttressing ice shelves and structural collapse of marine-terminating ice cliffs—that is calibrated against Pliocene and Last Interglacial sea-level estimates and applied to future greenhouse gas emission scenarios. Antarctica has the potential to contribute more than a metre of sea-level rise by 2100 and more than 15 metres by 2500, if emissions continue unabated. In this case atmospheric warming will soon become the dominant driver of ice loss, but prolonged ocean warming will delay its recovery for thousands of years.

Reconstructions of the global mean sea level (GMSL) during past warm climate intervals including the Pliocene (about three million years ago)[1] and late Pleistocene interglacials[2–5] imply that the Antarctic ice sheet has considerable sensitivity. Pliocene atmospheric CO_2 concentrations were comparable to today's (~400 parts per million by volume, p.p.m.v.)[6], but some sea-level reconstructions are 10–30 m higher[1,7]. In addition to the loss of the Greenland Ice Sheet and the West Antarctic Ice Sheet (WAIS)[2], these high sea levels require the partial retreat of the East Antarctic Ice Sheet (EAIS), which is further supported by sedimentary evidence from the Antarctic margin[8]. During the more recent Last Interglacial (LIG, 130,000 to 115,000 years ago), GMSL was 6–9.3 m higher than it is today[2–4], at a time when atmospheric CO_2 concentrations were below 280 p.p.m.v. (ref. 9) and global mean temperatures were only about 0–2 °C warmer[10]. This requires a substantial sea-level contribution from Antarctica of 3.6–7.4 m in addition to an estimated 1.5–2 m from Greenland[11,12] and around 0.4 m from ocean steric effects[10]. For both the Pliocene and the LIG, it is difficult to obtain the inferred sea-level values from ice-sheet models used in future projections.

Marine ice sheet and ice cliff instabilities

Much of the WAIS sits on bedrock hundreds to thousands of metres below sea level (Fig. 1a)[13]. Today, extensive floating ice shelves in the Ross and Weddell Seas, and smaller ice shelves and ice tongues in the Amundsen and Bellingshausen seas (Fig. 1b) provide buttressing that impedes the seaward flow of ice and stabilizes marine grounding zones (Fig. 2a). Despite their thickness (typically about 1 km near the grounding line to a few hundred metres at the calving front), a warming ocean has the potential to quickly erode ice shelves from below, at rates exceeding 10 m yr^{-1} $°C^{-1}$ (ref. 14). Ice-shelf thinning and reduced backstress enhance seaward ice flow, grounding-zone thinning, and retreat (Fig. 2b). Because the flux of ice across the grounding line increases strongly as a function of its thickness[15], initial retreat onto a reverse-sloping bed (where the bed deepens and the ice thickens upstream) can trigger a runaway Marine Ice Sheet Instability (MISI; Fig. 2c)[15–17]. Many WAIS grounding zones sit precariously on the edge of such reverse-sloped beds, but the EAIS also contains deep subglacial basins with reverse-sloping, marine-terminating outlet troughs up to 1,500 m deep (Fig. 1). The ice above floatation in these East Antarctic basins is much thicker than in West Antarctica, with the potential to raise GMSL by around 20 m if the ice in those basins is lost[13]. Importantly, previous ice-sheet simulations accounting for migrating grounding lines and MISI dynamics have shown the potential for repeated WAIS retreats and readvances over the past few million years[18], but could only account for GMSL rises of about 1 m during the LIG and 7 m in the warm Pliocene, which are substantially smaller than geological estimates.

So far, the potential for MISI to cause ice-sheet retreat has focused on the role of ocean-driven melting of buttressing ice shelves from below[16,18–20]. However, it is often overlooked that the major ice shelves in the Ross and Weddell seas and the many smaller shelves and ice tongues buttressing outlet glaciers are also vulnerable to atmospheric warming. Today, summer temperatures approach or just exceed 0 °C on many shelves[21], and their flat surfaces near sea level mean that little atmospheric warming would be needed to dramatically increase the areal extent of surface melting and summer rainfall.

Meltwater on ice-shelf surfaces causes thinning if it percolates through the shelf to the ocean. If refreezing occurs, the ice is warmed, reducing its viscosity and speeding its flow[22]. The presence of rain and meltwater can also influence crevassing and calving rates[23] (hydrofracturing) as witnessed on the Antarctic Peninsula's Larson B ice shelf during its sudden break-up in 2002[24]. Similar dynamics could have affected the ice sheet during ancient warm intervals[25], and given enough future warming, could eventually affect many ice shelves and ice tongues, including the major buttressing shelves in the Ross and Weddell seas.

Another physical mechanism previously underappreciated at the ice-sheet scale involves the mechanical collapse of ice cliffs in places where marine-terminating ice margins approach 1 km in thickness, with >90 m of vertical exposure above sea level[26]. Today, most Antarctic outlet glaciers with deep beds approaching a water depth of 1 km are protected by buttressing ice shelves, with gently sloping surfaces at the grounding line (Fig. 2d). However, given enough atmospheric warming above or ocean warming below (Fig. 2e), ice-shelf retreat can outpace its dynamically accelerated seaward flow as buttressing is lost and

[1]Department of Geosciences, University of Massachusetts, Amherst, Massachusetts 01003, USA. [2]Earth and Environmental Systems Institute, Pennsylvania State University, University Park, Pennsylvania 16802, USA.

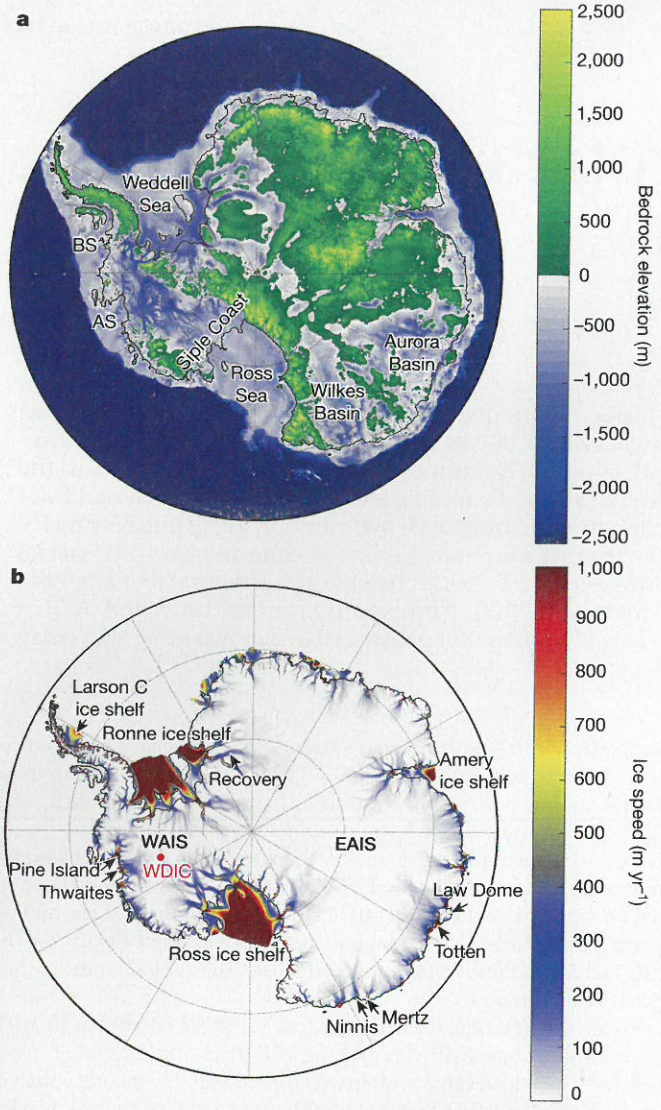

Figure 1 | Antarctic sub-glacial topography and ice sheet features. **a**, Bedrock elevations[13] interpolated onto the 10-km polar stereographic ice-sheet model grid and used in Pliocene, LIG, and future ice-sheet simulations. **b**, Model surface ice speeds and grounding lines (black lines) show the location of major ice streams, outlet glaciers, and buttressing ice shelves (seaward of grounding lines) relative to the underlying topography in **a**. Features and place names mentioned in the text are also shown. AS, Amundsen Sea; BS, Bellingshausen Sea; WDIC, WAIS Divide Ice Core. The locations of the Pine Island, Thwaites, Ninnis, Mertz, Totten, and Recovery glaciers are shown. Model ice speeds (**b**) are shown after equilibration with a modern atmospheric and ocean climatology (see Methods).

retreating grounding lines thicken[15]. In places where marine-terminating grounding lines are thicker than 800 m or so, this would produce >90 m subaerial cliff faces that would collapse (Fig. 2f) simply because longitudinal stresses at the cliff face would exceed the yield strength (about 1 MPa) of the ice[26].

More heavily crevassed and damaged ice would reduce the maximum supported cliff heights. If a thick, marine-terminating grounding line began to undergo such mechanical failure, its retreat would continue unabated until temperatures cooled enough to reform a buttressing ice shelf, or the ice margin retreated onto bed elevations too shallow to support the tall, unstable cliffs[25]. If protective ice shelves were suddenly lost in the vast areas around the Antarctic margin where reverse-sloping bedrock is more than 1,000 m deep (Fig. 1a), exposed grounding-line ice cliffs would quickly succumb to structural failure, as is happening in the few places where such conditions exist today (the Helheim and Jakobsavn glaciers on Greenland and the Crane Glacier on the Antarctic Peninsula), hinting that a Marine Ice Cliff Instability (MICI) in addition to MISI could be an important contributor to past and future ice-sheet retreat.

Our three-dimensional ice sheet–ice shelf model[25,27] (Methods) predicts the evolution of continental ice thickness and temperature as a function of ice flow (deformation and sliding) and changes in mass balance via precipitation, runoff, basal melt, oceanic melt under ice shelves and on vertical ice faces, calving, and tidewater ice-cliff failure. The model captures MISI (Fig. 2a–c) by accounting for migrating grounding lines and the buttressing effects of ice shelves with pinning points and side-shear. To capture the dynamics of MICI (Fig. 2d–f), new physical treatments of surface-melt and rainwater-enhanced calving (hydrofracturing) and grounding-line ice-cliff dynamics have been added[25]. Including these processes was found to increase the model's contribution to Pliocene GMSL from +7 m (ref. 18) to +17 m (ref. 25). The model formulation used here is similar to that described in ref. 25, but with improvements in the treatment of calving, thermodynamics, and climate–ice–ocean coupling (Methods).

The Antarctic Ice Sheet in the Pliocene

The warm mid-Pliocene and LIG provide complementary targets for model performance, via the ability to produce ~5–20 m and ~3.5–7.5 m GMSL from Antarctica, respectively. These two time periods highlight model sensitivities to different processes, because Pliocene summer air temperatures were capable of producing substantial surface meltwater, especially during warm austral summer orbits[28]. Conversely, LIG temperatures were cooler[29], with limited potential for surface meltwater production. Instead, ocean temperatures[30] could have been the determining factor in LIG ice retreat[31].

To simulate Pliocene and LIG ice sheets, we couple the ice model to a high-resolution, atmospheric regional climate model (RCM) adapted to Antarctica and nested within a global climate model (GCM; see Methods). The RCM captures the orographic details of ice shelves and adjacent ice-sheet margins, which is critical here because the new calving and grounding line processes are mechanistically linked to the atmosphere.

High-resolution ocean modelling beneath time-evolving ice shelves on palaeoclimate timescales exceeds existing capabilities. Instead, we use a modern ocean climatology[32] interpolated to our ice-sheet grid, with uniformly imposed sub-surface ocean warming providing melt rates on sub-ice-shelf and calving-front surfaces exposed to sea water. The RCM climatologies and imposed ocean warming are applied to quasi-equilibrated initial ice-sheet states, with atmospheric temperatures and the precipitation lapse-rate corrected as the ice sheet evolves.

As in ref. 25, the Pliocene simulation uses a RCM climatology with 400 p.p.m.v. CO_2, a warm austral summer orbit[28], and 2 °C imposed ocean warming to represent maximum mid-Pliocene warmth (Extended Data Fig. 1). The model produces an 11.3-m contribution to GMSL rise, reflecting a reduction in its sensitivity of about 6 m relative to the formulation in ref. 25, but within the range of plausible sea-level estimates[1,7]. Pliocene retreat is triggered by meltwater-induced hydrofracturing of ice shelves, which relieves backstress and initiates both MISI and MICI retreat into the deepest sectors of WAIS and EAIS marine basins.

The Antarctic Ice Sheet during the LIG

Summer air temperatures in the RCM are slightly warmer at 116 kyr ago than 128 kyr ago, but remain below freezing in both cases, with little to no surface melt (Extended Data Fig. 2). As a result, substantial oceanic warming >4 °C is required to initiate WAIS retreat at 128 kyr ago, which occurs once an ocean-melt threshold is reached in the stability of the Thwaites grounding line (Extended Data Fig. 3a and d). Allowing two-way coupling between the RCM and the ice-sheet model

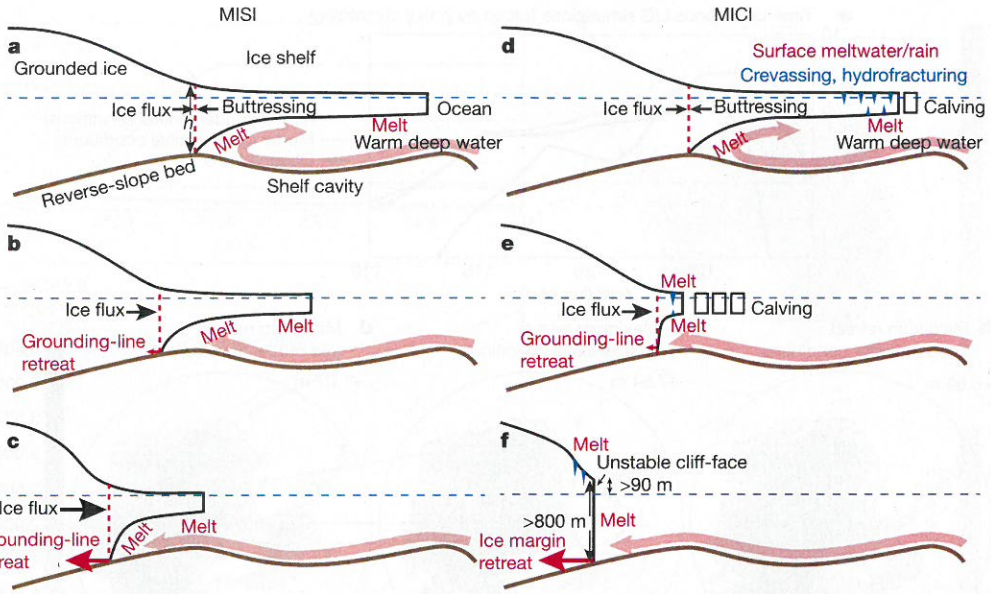

Figure 2 | Schematic representation of MISI and MICI and processes included in the ice model. Top-to-bottom sequences (**a**–**c** and **d**–**f**) show progressive ice retreat into a subglacial basin, triggered by oceanic and atmospheric warming. The pink arrow represents the advection of warm circumpolar deep water (CDW) into the shelf cavity. **a**, Stable, marine-terminating ice-sheet margin, with a buttressing ice shelf. Seaward ice flux is strongly dependent on grounding-line thickness h. Sub-ice melt rates increase with open-ocean warming and warm-water incursions into the ice-shelf cavity. **b**, Thinning shelves and reduced buttressing increase seaward ice flux, backing the grounding line onto reverse-sloping bedrock. **c**, Increasing h with landward grounding-line retreat leads to an ongoing increase in ice flow across the grounding line in a positive runaway feedback until the bed slope changes. **d**, In addition to MISI (**a**–**c**), the model physics used here account for surface-meltwater-enhanced calving via hydrofracturing of floating ice (**e**), providing an additional mechanism for ice-shelf loss and initial grounding-line retreat into deep basins. **f**, Where oceanic melt and enhanced calving eliminate shelves completely, subaerial cliff faces at the ice margin become structurally unstable where h exceeds 800 m, triggering rapid, unabated MICI retreat into deep basins.

(Methods) captures dynamical atmospheric feedbacks as the ice margin retreats. This enhances retreat (Extended Data Fig. 3b, e), but still requires >4 °C of ocean warming to produce a >3.5 m increase in GMSL. We find that by accounting for the additional influence of circum-Antarctic ocean warming on the RCM atmosphere (Methods), the GMSL contribution increases to >6.5 m with just 3 °C sub-surface ocean warming (Extended Data Fig. 3c and f), despite the cooler orbit of the Earth 128 kyr ago. The ocean-driven continental warming at 128 kyr ago agrees with ice core records[29] and supports a Southern Ocean control on the timing of ice-sheet retreat[30,31], possibly through Northern Hemisphere influences on the ocean meridional overturning circulation[33].

Alternative simulations (Fig. 3) use time-evolving atmospheric and oceanic climatologies (Methods) based on marine and ice-core proxy reconstructions[29]. These time-continuous simulations produce GMSL contributions of 6–7.5 m early in the interglacial, followed by a prolonged plateau and rapid recovery of the ice sheet beginning around 115 kyr ago. This result matches the magnitude, temporal pattern, and rate of LIG sea-level change in ref. 3. (Fig. 3a), and the simulated recovery of the WAIS satisfies the presence of ice >70 kyr ago at the bottom of the WAIS Divide Ice Core[34].

Combined with estimates of Greenland ice loss[11,12,35] and ocean thermal effects[10], the simulated, Antarctic contributions to Pliocene and LIG sea level are in much better agreement with geological estimates[2–4] than previous versions of our model[18,27], which lacked these new treatments of meltwater-enhanced calving and ice-margin dynamics, suggesting that the new model is better suited to simulations of future ice response.

Future simulations

Using the same model physics and parameter values as used in the Pliocene and LIG simulations, we apply the ice-sheet model to long-term future simulations (Methods). Here, atmospheric forcing is provided by high-resolution RCM simulations (Extended Data Fig. 4) following three extended Representative Carbon Pathway (RCP) scenarios (RCP2.6, RCP4.5 and RCP8.5)[36]. Future circum-Antarctic ocean temperatures used in our time-evolving sub-ice melt-rate calculations come from matching, high-resolution (1°) National Center for Atmospheric Research (NCAR) CCSM4 simulations (ref. 37, Extended Data Fig. 5). The simulations begin in 1950 to provide some hindcast spinup, and are run for 550 years to 2500.

The RCP scenarios (Fig. 4) produce a wide range of future Antarctic contributions to sea level, with RCP2.6 producing almost no net change by 2100, and only 20 cm by 2500. Conversely, RCP4.5 causes almost complete WAIS collapse within the next five hundred years, primarily owing to the retreat of Thwaites Glacier into the deep WAIS interior. The Siple Coast grounding zone remains stable until late in the simulation, thanks to the persistence of the buttressing Ross Ice Shelf (see Supplementary Video 2). In RCP4.5, GMSL rise is 32 cm by 2100, but subsequent retreat of the WAIS interior, followed by the fringes of the Wilkes Basin and the Totten Glacier/Law Dome sector of the Aurora Basin produces 5 m of GMSL rise by 2500.

In RCP8.5, increased precipitation causes an initial, minor gain in total ice mass (Fig. 4d), but rapidly warming summer air temperatures trigger extensive surface meltwater production[38] and hydrofracturing of ice shelves by the middle of this century (Extended Data Fig. 4). The Larsen C is one of the first shelves to be lost, about 2055. Around the same time, major thinning and retreat of outlet glaciers commences in the Amundsen Sea Embayment, beginning with Pine Island Glacier (Fig. 4h), and along the Bellingshausen margin. Massive meltwater production on shelf surfaces, and eventually on the flanks of the ice sheet, would quickly overcome the buffering capacity of firn[39]. In the model, the meltwater accelerates WAIS retreat via its thermomechanical influence on ice rheology (Methods) and the influence of hydrofacturing on crevassing and structural failure of the retreating margin. Antarctica contributes 77 cm of GMSL rise by 2100, and continued loss of the Ross and Weddell Sea ice shelves drives WAIS retreat from three sides simultaneously (the Amundsen, Ross, and Weddell seas), all with

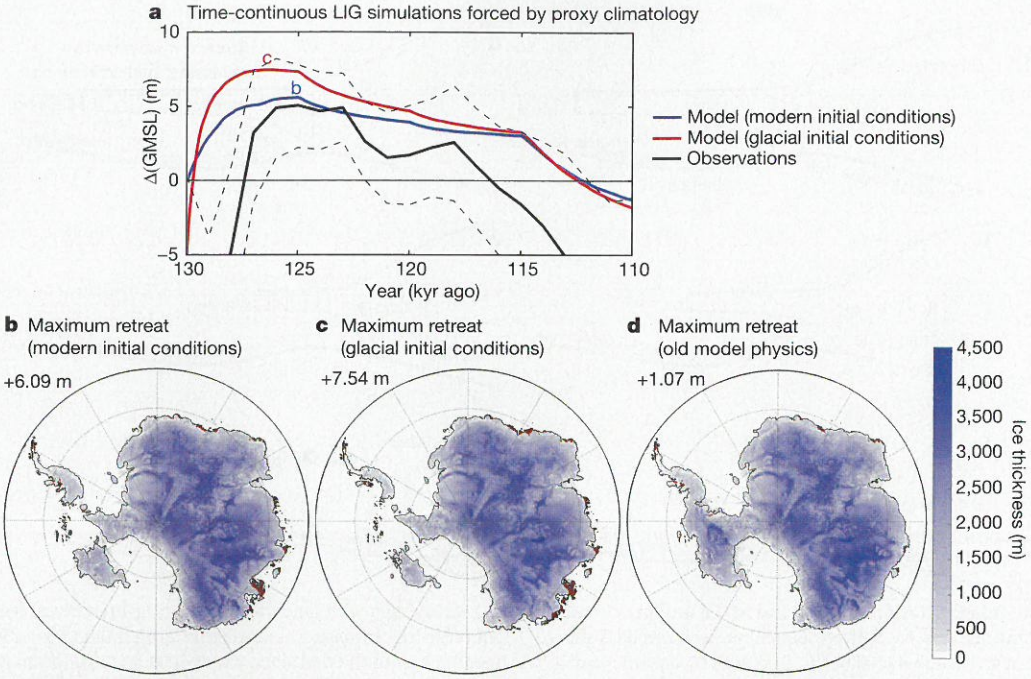

Figure 3 | Ice-sheet simulations and Antarctic contributions to GMSL through the LIG driven by a time-evolving, proxy-based atmosphere–ocean climatology. a, Change in GMSL in LIG simulations starting at 130 kyr ago and initialized with a modern ice sheet (blue) or a bigger LGM ice sheet representing glacial conditions at the onset of the LIG (red). A probabilistic reconstruction of Antarctica's contribution to GMSL is shown in black[3] with uncertainties (16th and 84th percentiles) as dashed lines. **b**, **c**, Ice-sheet thickness at the time of maximum retreat using modern initial conditions (**b**) and using glacial initial conditions (**c**). Ice-free land surfaces are brown. The bigger sea-level response when initialized with the 'glacial' ice sheet is caused by deeper bed elevations and the ~3,000-yr lagged bedrock response to ice retreat[50], which enhances bathymetrically sensitive MISI dynamics. **d**, The same simulation as **b** without the new model physics accounting for meltwater-enhanced calving or ice-cliff failure[27]. GMSL contributions are shown at top left.

reverse-sloping beds into the deep ice-sheet interior. As a result, WAIS collapses within 250 years. At the same time, steady retreat into the Wilkes and Aurora basins, where the ice above floatation is >2,000 m thick, adds substantially to the rate of sea-level rise, exceeding 4 cm yr^{-1} (Fig. 4c) in the next century, which is comparable to maximum rates of sea-level rise during the last deglaciation[40]. At 2500, GMSL rise for the RCP8.5 scenario is 12.3 m. As in our LIG simulations, atmosphere–ice sheet coupling accounting for the warming feedback associated with the retreating ice sheet adds an additional 1.3 m of GMSL to the RCP8.5 scenario (Fig. 4b).

The CCSM4 simulations providing the model's sub-ice-shelf melt rates (Extended Data Fig. 5) underestimate the penetration of warm Circum-Antarctic Deep Water into the Amundsen and Bellingshausen seas observed in recent decades[41]. As a result, the model fails to capture recent, 21st-century thinning and grounding-line retreat along the southern Antarctic Peninsula[42] and the Amundsen Sea Embayment[43]. Correcting for the ocean-model cool bias along this sector of coastline improves the position of Pine Island and Thwaites grounding lines relative to observations[42,43] (Fig. 4h) and increases GMSL rise by 9 cm at 2100 (mainly due to the accelerated retreat of Pine Island Glacier), but the correction has little effect on longer timescales (Extended Data Table 1). Ocean warming is important to the behaviour of individual outlet glaciers early in the simulations, but we find that most of the long-term sea-level rise in RCP4.5 and RCP8.5 scenarios is caused by atmospheric warming and the onset of extensive surface meltwater production, rather than ocean warming as implied by other recent studies[44–46]. Without atmospheric warming, the magnitude of RCP8.5 ocean warming in CCSM4 is insufficient to cause the major retreat of the WAIS or East Antarctic basins; and even with >3 °C additional warming in the Amundsen and Bellingshausen seas it takes several thousand years for WAIS to retreat via ocean-driven MISI dynamics alone (Extended Data Fig. 6). We note that despite the 10-km grid resolution, the model simulates major ice streams well (Fig. 1), including their internal variability[18]. However, during drastic subglacial-basin retreat the internal variability is quickly overtaken as grounding lines recede into deep interior catchments (see Supplementary Video 10).

Large Ensemble analysis

To better utilize Pliocene and LIG geological constraints on model performance, we perform a Large Ensemble analysis (Methods) to explore the uncertainty associated with the primary parameter values controlling (1) relationships between ocean temperature and sub-ice-shelf melt rates, (2) hydrofracturing (crevasse penetration in relation to surface liquid water supply), and (3) maximum rates of marine-terminating ice-cliff failure. The combination of Pliocene and LIG sea level targets is ideal, because Pliocene retreat is dominated by processes associated with (2) and (3), while the LIG is dominated by process (1).

Both Pliocene and LIG ensembles are run with combinations of widely ranging parameter values associated with the three processes, and the combinations are scored by their ability to simulate target ranges of Pliocene and LIG Antarctic sea-level contributions (Methods). The filtered subsets of parameter values capable of reproducing both targets are then used in ensembles of future RCP scenarios (Extended Data Table 2), providing both an envelope of possible outcomes and an estimate of the model's parametric uncertainty (Fig. 5). Importantly, the ensemble analysis supports our choice of 'default' model parameters used in the nominal Pliocene, LIG, and future simulations (Fig. 4, Extended Data Table 2). The lack of substantial ice-sheet retreat in the optimistic RCP2.6 scenario remains unchanged, but the Large Ensemble analysis substantially increases our RCP4.5 and RCP8.5 2100 sea-level projections to 49 ± 20 cm and 105 ± 30 cm, if higher (>10 m instead of >5 m) Pliocene sea-level targets are used. Adding the ocean temperature correction in the Amundsen and Bellingshausen seas (Fig. 4d and h) further increases the 2100 projections in RCP2.6, RCP4.5 and RCP8.5 to 16 ± 16 cm, 58 ± 28 cm and 114 ± 36 cm, respectively (see Methods and Extended Data Tables 1 and 2).

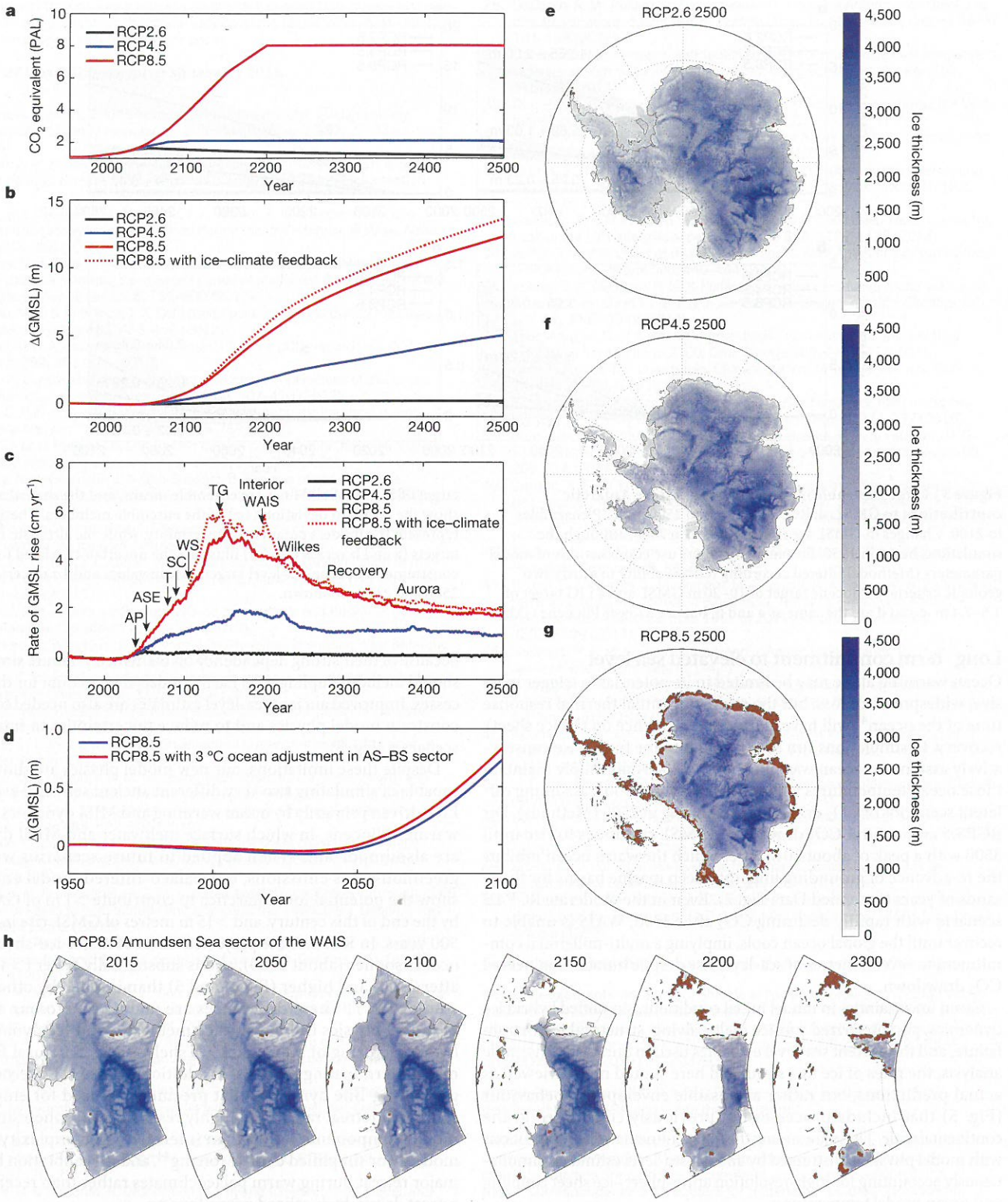

Figure 4 | Future ice-sheet simulations and Antarctic contributions to GMSL from 1950 to 2500 driven by a high-resolution atmospheric model and 1° NCAR CCSM4 ocean temperatures. a, Equivalent CO_2 forcing applied to the simulations, following the RCP emission scenarios in ref. 36, except limited to 8 × PAL (preindustrial atmospheric level, where 1 PAL = 280 p.p.m.v.). **b**, Antarctic contribution to GMSL. **c**, Rate of sea-level rise and approximate timing of major retreat and thinning in the Antarctic Peninsula (AP), Amundsen Sea Embayment (ASE) outlet glaciers, AS–BS, Amundsen Sea–Bellingshausen Sea; the Totten (T), Siple Coast (SC) and Weddell Sea (WS) grounding zones, the deep Thwaites Glacier basin (TG), interior WAIS, the Recovery Glacier, and the deep EAIS basins (Wilkes and Aurora). **d**, Antarctic contribution to GMSL over the next 100 years for RCP8.5 with and without a +3 °C adjustment in ocean model temperatures in the Amundsen and Bellingshausen seas as shown in Extended Data Fig. 5d. **e–g**, Ice-sheet snapshots at 2500 in the RCP2.6 (**e**), RCP4.5 (**f**) and RCP8.5 (**g**) scenarios. Ice-free land surfaces are shown in brown. **h**, Close-ups of the Amundsen Sea sector of WAIS in RCP8.5 with bias-corrected ocean model temperatures.

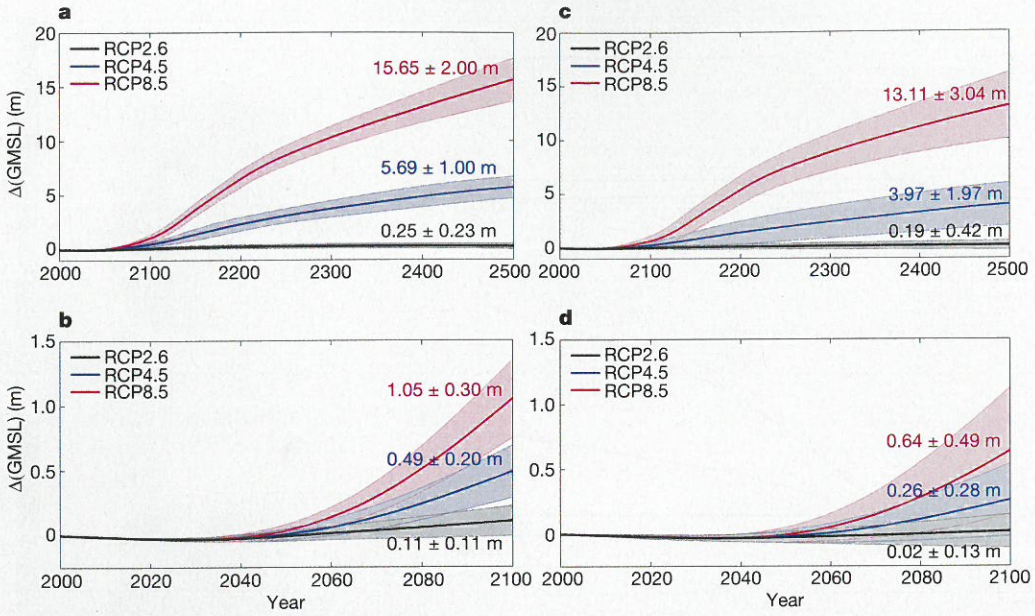

Figure 5 | Large Ensemble model analyses of future Antarctic contributions to GMSL. a, RCP ensembles to 2500. **b**, RCP ensembles to 2100. Changes in GMSL are shown relative to 2000, although the simulations begin in 1950. Ensemble members use combinations of model parameters (Methods) filtered according to their ability to satisfy two geologic criteria: a Pliocene target of 10–20 m GMSL and a LIG target of 3.6–7.4 m. **c** and **d** are the same as **a** and **b**, but use a lower Pliocene GMSL target of 5–15 m. Solid lines are ensemble means, and the shaded areas show the standard deviation (1σ) of the ensemble members. The 1σ ranges represent the model's parametric uncertainty, while the alternate Pliocene targets (**a** and **b** versus **c** and **d**) illustrate the uncertainty related to poorly constrained Pliocene sea-level targets. Mean values and 1σ uncertainties at 2500 and 2100 are shown.

Long-term commitment to elevated sea level

Ocean warming alone may be limited in its potential to trigger massive, widespread ice loss, but the multi-millennial thermal response time of the ocean[47] will have a profound influence on the ice sheet's recovery. In simulations run 5,000 years into the future, we conservatively assume no ocean warming beyond 2300 and simply maintain those ocean temperatures while the atmosphere cools assuming different scenarios of CO_2 drawdown beginning in 2500 (Methods). For RCP8.5 and natural CO_2 drawdown, GMSL continues to rise until 3500 with a peak of about 20 m, after which the warm ocean inhibits the re-advance of grounding lines into deep marine basins for thousands of years (Extended Data Fig. 7). Even in the moderate RCP4.5 scenario with rapidly declining CO_2 after 2500, WAIS is unable to recover until the global ocean cools, implying a multi-millennial commitment to several metres of sea-level rise despite human-engineered CO_2 drawdown.

Given uncertainties in model initial conditions, simplified hybrid ice dynamics, parameterized sub-ice melt, calving, structural ice-margin failure, and the ancient sea-level estimates used in our Large Ensemble analysis, the rates of ice loss simulated here should not be viewed as actual predictions, but rather as possible envelopes of behaviour (Fig. 5) that include processes not previously considered at the continental scale. These are among the first continental-scale simulations with model physics constrained by ancient sea-level estimates, simultaneously accounting for high-resolution atmosphere–ice sheet coupling and ocean model temperatures.

However, several important processes are lacking and should be included in future work. In particular, the model lacks two-way coupling between the ice sheet and the ocean. This is especially relevant for RCP8.5, in which >1 Sv of freshwater and icebergs would be supplied to the Southern Ocean during peak retreat (Extended Data Fig. 8). Rapid calving and ice-margin collapse also implies ice mélange in restricted embayments that could provide buttressing and a negative feedback on retreat. The loss of ice mass would also have a strong effect on relative sea level at the margin owing to gravitational and solid-earth deformation effects[48], which could affect MISI and MICI dynamics because of their strong dependency on bathymetry. Future simulations should include coupling with Earth models that account for these processes. Improved ancient sea-level estimates are also needed to further constrain model physics and to reduce uncertainties in future RCP scenarios (Fig. 5).

Despite these limitations, our new model physics are shown to be capable of simulating two very different ancient sea-level events: the LIG, driven primarily by ocean warming and MISI dynamics, and the warmer Pliocene, in which surface meltwater and MICI dynamics are also important. When applied to future scenarios with high greenhouse gas emissions, our palaeo-filtered model ensembles show the potential for Antarctica to contribute >1 m of GMSL rise by the end of this century, and >15 m metres of GMSL rise in the next 500 years. In RCP8.5, the projected onset of major ice-sheet retreat occurs sooner (about 2050), and is substantially faster (>4 cm yr^{-1} after 2100) and higher (Figs 4 and 5) than implied by other recent studies[44,45,49]. These differences are mainly due to our addition of model physics linking surface meltwater and ice dynamics via hydrofracturing of buttressing ice shelves and structural failure of marine-terminating ice cliffs. In addition, we use (1) freely evolving grounding-line dynamics that preclude the need for empirically calibrated retreat rates[49], (2) highly resolved atmosphere and ocean model components rather than intermediate-complexity climate models[45] or simplified climate forcing[44], and (3) calibration based on major retreat during warm palaeoclimates rather than recent minor retreat driven by localized ocean forcing.

As in these prior studies, we also find that ocean-driven melt is an important driver of grounding-line retreat where warm water is in contact with ice shelves, but in scenarios with high greenhouse gas emissions we find that atmospheric warming soon overtakes the ocean as the dominant driver of Antarctic ice loss. Surface meltwater may lead to the ultimate demise of the major buttressing ice shelves (Supplementary Videos 8 and 9) and extensive grounding-line retreat, but it is the long thermal memory of the ocean that will inhibit the recovery of marine-based ice for thousands of years after greenhouse gas emissions are curtailed.

Online Content Methods, along with any additional Extended Data display items and Source Data, are available in the online version of the paper; references unique to these sections appear only in the online paper.

Received 27 May 2015; accepted 12 January 2016.

1. Rovere, A. *et al.* The Mid-Pliocene sea-level conundrum: glacial isostasy, eustasy and dynamic topography. *Earth Planet. Sci. Lett.* **387,** 27–33 (2014).
2. Dutton, A. *et al.* Sea-level rise due to polar ice-sheet mass loss during past warm periods. *Science* **3491,** http://dx.doi.org/10.1126/science.aaa4019 (2015).
3. Kopp, R. E., Simons, F. J., Mitrovica, J. X., Maloof, A. C. & Oppenheimer, M. Probabilistic assessment of sea level during the last interglacial stage. *Nature* **462,** 863–868 (2009).
4. O'Leary, M. J., Hearty, P. J., Thompson, W. G., Raymo, M. E. & Mitrovica, J. X. Ice sheet collapse following a prolonged period of stable sea level during the last interglacial. *Nature Geosci.* **6,** 796–800 (2013).
5. Raymo, M. E. & Mitrovica, J. X. Collapse of polar ice sheets during the stage 11 interglacial. *Nature* **483,** 453–456 (2012).
6. Seki, O. *et al.* Alkenone and boron-based Pliocene pCO_2 records. *Earth Planet. Sci. Lett.* **292,** 201–211 (2010).
7. Miller, K. G. *et al.* High tide of the warm Pliocene: implications of global sea level for Antarctic deglaciation. *Geology* **40,** 407–410 (2012).
8. Cook, C. P. *et al.* Dynamic behaviour of the East Antarctic ice sheet during Pliocene warmth. *Nature Geosci.* **6,** 765–769 (2013).
9. Lüthi, D. *et al.* High-resolution carbon dioxide concentration record 650,000–800,000 years before present. *Nature* **453,** 379–382 (2008).
10. McKay, N. P., Overpeck, J. & Otto-Bliesner, B. The role of ocean thermal expansion in Last Interglacial sea level rise. *Geophys. Res. Lett.* **38,** L14605 (2011).
11. NEEM community members. Eemian interglacial reconstructed from a Greenland folded ice core. *Nature* **493,** 489–494 (2013).
12. Stone, E. J., Lunt, D. J., Annan, J. D. & Hargreaves, J. C. Quantification of the Greenland ice sheet contribution to Last Interglacial sea level rise. *Clim. Past* **9,** 621–639 (2013).
13. Fretwell, P. *et al.* Bedmap2: improved ice bed, surface and thickness datasets for Antarctica. *Cryosphere* **7,** 375–393 (2013).
14. Shepherd, A., Wingham, D. & Rignot, E. Warm ocean is eroding West Antarctic Ice Sheet. *Geophys. Res. Lett.* **31,** L23402 (2004).
15. Schoof, C. Ice sheet grounding line dynamics: steady states, stability, and hysteresis. *J. Geophys. Res.* **112,** F03S28 (2007).
16. Favier, L. *et al.* Retreat of Pine Island Glacier controlled by marine ice-sheet instability. *Nature Geosci.* **7,** 874–878 (2014).
17. Mercer, J. H. West Antarctic Ice Sheet and CO_2 greenhouse effect—threat of disaster. *Nature* **271,** 321–325 (1978).
18. Pollard, D. & DeConto, R. M. Modeling West Antarctic Ice Sheet growth and collapse through the last 5 million years. *Nature* **458,** 329–332 (2009).
19. Pritchard, H. D. *et al.* Antarctic ice-sheet loss driven by basal melting of ice shelves. *Nature* **484,** 502–505 (2012).
20. Joughin, I., Smith, B. E. & Medley, B. Marine ice sheet collapse potentially under way for the Thwaites Glacier basin, West Antarctica. *Science* **344,** 735–738 (2014).
21. Tedesco, M. & Monaghan, A. J. An updated Antarctic melt record through 2009 and its linkages to high-latitude and tropical climate variability. *Geophys. Res. Lett.* **36,** L18502 (2009).
22. Phillips, T., Rajraram, H. & Steffen, K. Cryo-hydrologic warming: a potential mechanism for rapid thermal response of ice sheets. *Geophys. Res. Lett.* **37,** L20503 (2010).
23. Nick, F. M., Van der Veen, C. J., Vieli, A. & Benn, D. I. A physically based calving model applied to marine outlet glaciers and implications for the glacier dynamics. *J. Glaciol.* **56,** 781–794 (2010).
24. Banwell, A. F., MacAyeal, D. R. & Sergienko, O. V. Breakup of the Larsen B Ice Shelf triggered by chain reaction drainage of supraglacial lakes. *Geophys. Res. Lett.* **40,** 5872–5876 (2013).
25. Pollard, D., DeConto, R. M. & Alley, R. B. Potential Antarctic Ice Sheet retreat driven by hydrofracturing and ice cliff failure. *Earth Planet. Sci. Lett.* **412,** 112–121 (2015).
26. Bassis, J. N. & Walker, C. C. Upper and lower limits on the stability of calving glaciers from the yield strength envelope of ice. *Proc. R. Soc. Lond. A* **468,** 913–931 (2012).
27. Pollard, D. & DeConto, R. Description of a hybrid ice sheet-shelf model, and application to Antarctica. *Geosci. Model Dev.* **5,** 1273–1295 (2012).
28. DeConto, R. M., Pollard, D. & Kowalewski, D. Modeling Antarctic ice sheet and climate variations during Marine Isotope Stage 31. *Glob. Planet. Change* **96–97,** 181–188 (2012).
29. Capron, E. *et al.* Temporal and spatial structure of multi-millennial temperature changes at high latitudes during the Last Interglacial. *Quat. Sci. Rev.* **103,** 116–133 (2014).
30. Duplessy, J. C., Roche, D. M. & Kageyama, M. The deep ocean during the Last Interglacial period. *Science* **316,** 89–91 (2007).
31. Overpeck, J. T. *et al.* Paleoclimatic evidence for future ice-sheet instability and rapid sea-level rise. *Science* **311,** 1747–1750 (2006).
32. Levitus, S. *et al.* World ocean heat content and thermosteric sea level change (0–2000 m), 1955–2010. *Geophys. Res. Lett.* **39,** http://dx.doi.org/10.1029/2012GL051106 (2012).
33. Galaasen, E. V. *et al.* Rapid reductions in North Atlantic Deep Water during the peak of the Last Interglacial period. *Science* **343,** 1129–1132 (2014).
34. Fudge, T. J. *et al.* Onset of deglacial warming in West Antarctica driven by local orbital forcing. *Nature* **500,** 440–444 (2013).
35. Koenig, S. J., DeConto, R. M. & Pollard, D. Impact of reduced Arctic sea ice on Greenland ice sheet variability in warmer than present climate. *Geophys. Res. Lett.* **41,** 3933–3942 (2014).
36. Meinshausen, N. *et al.* The RCP greenhouse gas concentrations and their extensions from 1765 to 2300. *Clim. Change* **109,** 213–241 (2011).
37. Gent, P. R. *et al.* The Community Climate System Model Version 4. *J. Clim.* **24,** 4973–4991 (2011).
38. Trusel, L. D. *et al.* Divergent trajectories of Antarctic surface melt under two twenty-first-century climate scenarios. *Nature Geosci.* **8,** 927–932 (2015).
39. Munneke, P. K., Ligtenberg, S. R. M., van den Broeke, M. R. & Vaughan, D. G. Firn air depletion as a precursor of Antarctic ice-shelf collapse. *J. Glaciol.* **60,** 205–214 (2014).
40. Carlson, A. E. & Clark, P. U. Ice sheet sources of sea level rise and freshwater discharge during the last deglaciation. *Rev. Geophys.* **50,** RG4007 (2012).
41. Schmidtko, S., Heywood, K. J., Thompson, A. F. & Aoki, S. Multidecadal warming of Antarctic waters. *Science* **346,** 1227–1231 (2014).
42. Wouters, B. *et al.* Dynamic thinning of glaciers on the Southern Antarctic Peninsula. *Science* **348,** 899–903 (2015).
43. Rignot, E., Mouginot, J., Morlighem, M., Seroussi, H. & Scheuchl, B. Widespread, rapid grounding line retreat of Pine Island, Thwaites, Smith, and Kohler glaciers, West Antarctica, from 1992 to 2011. *Geophys. Res. Lett.* **41,** 3502–3509 (2014).
44. Golledge, N. R. *et al.* The multi-millennial Antarctic commitment to future sea-level rise. *Nature* **526,** 421–425 (2015).
45. Winkelmann, R., Levermann, A., Ridgwell, A. & Caldeira, K. Combustion of available fossil fuel resources sufficient to eliminate the Antarctic Ice Sheet. *Sci. Adv.* **1,** e1500589 (2015).
46. Feldmann, J. & Levermann, A. Collapse of the West Antarctic Ice Sheet after local destabilization of the Amundsen Basin. *Proc. Natl Acad. Sci.* **112,** 14191–14196 (2015).
47. Li, C., von Storch, J.-S. & Marotzke, J. Deep-ocean heat uptake and equilibrium climate response. *Clim. Dyn.* **40,** 1071–1086 (2013).
48. Gomez, N., Pollard, D. & Holland, D. Sea-level feedback lowers projections of future Antarctic Ice-Sheet mass loss. *Nature Commun.* **6,** 8798, http://dx.doi.org/10.1038/ncomms9798 (2015).
49. Ritz, C. *et al.* Potential sea-level rise from Antarctic ice-sheet instability constrained by observations. *Nature* **528,** 115–118 (2015).
50. Huybrechts, P. *The Antarctic Ice Sheet and Environmental Change: a Three-dimensional Modelling Study* PhD thesis, http://epic.awi.de/1463/, Vrije Univ. Brussel (1992).

Supplementary Information is available in the online version of the paper.

Acknowledgements We thank C. Shields at NCAR for providing CCSM4 ocean model data. NCAR is sponsored by the NSF. We also thank R. Kopp for providing LIG sea-level data, and R. Alley, A. Dutton, and M. Raymo for discussions. This research was supported by the NSF under awards OCE 1202632 PLIOMAX project and AGS 1203910/1203792.

Author Contributions R.M.D. and D.P. conceived the model experiments, developed the models, and wrote the manuscript.

Author Information Reprints and permissions information is available at www.nature.com/reprints. The authors declare no competing financial interests. Readers are welcome to comment on the online version of the paper. Correspondence and requests for materials should be addressed to R.M.D. (deconto@geo.umass.edu).